

EFFECT OF TEMPERATURE AND PRINTING ANGLE IN FDM ADDITIVE PRINTING ON THE STRENGTH PROPERTIES OF PET-G

Patryk Krawulski^{1*}, Katarzyna Panasiuk², Mirosław Tylińczak³

^{1,2,3} Gdynia Maritime University, Morska 81-87, 81-225 Gdynia, Poland,
Faculty of Marine Engineering

¹ ORCID 0000-0002-7093-6627, e-mail: p.krawulski@wm.umg.edu.pl

² ORCID 0000-0002-7138-0827, e-mail: k.panasiuk@wm.umg.edu.pl

³ ORCID 0000-0001-7148-7803, e-mail: m.tylińczak@wm.umg.edu.pl

*Corresponding author

Abstract: 3D printing, also known as additive printing or additive manufacturing, has become an integral part of today's manufacturing technologies, enabling rapid and flexible fabrication of three-dimensional objects from a variety of materials. Its importance in many fields is steadily increasing due its capabilities in prototyping, custom manufacturing and product personalisation. With the development of 3D printing technology, it is increasingly being used in the manufacture of marine machine parts and equipment. Before such products are implemented for real-world use, they require a thorough analysis of strength properties. In this work, the strength properties of the PET-G material were analysed with a change in temperature and printing angle using FDM (fused deposition modelling). Preliminary analysis of the results identified the best printing angle setting and the optimum choice of printing temperature.

Keywords: 3D printing, FDM, PET-G, strength properties.

1. INTRODUCTION

3D printing, which is known as a form of additive manufacturing, is one of the most innovative technologies in modern engineering and manufacturing [Kumaresan et al. 2023]. In contrast to traditional decremental machining methods, which mainly rely on the removal of material from solids, 3D printing is layer-by-layer application (Fig. 1) of an appropriately selected material based on a previously prepared three-dimensional model [Fountas et al. 2022]. Additive manufacturing provides great design and production capabilities. It allows the fabrication of structures and complex shapes that were not previously attainable using traditional methods [Popescu et al. 2018].

Additive manufacturing gained popularity in the 1980s. However, the technology has seen real development in recent decades [Szykiedans, Credo and Osiński 2017]. Its significance continues to grow in a wide range of fields, from industry to medicine and the arts, due to its capability in rapid prototyping [Soleyman et al. 2022]. The 3D printing methods most commonly used are FDM (fused deposition modelling), SLS (selective laser sintering) and SLA (stereolithography). Each of the methods is based on different materials and technologies. FDM (Fig. 2) is one of the cheapest and simplest additive manufacturing techniques [Zisopol, Minescu and Iacob 2023].

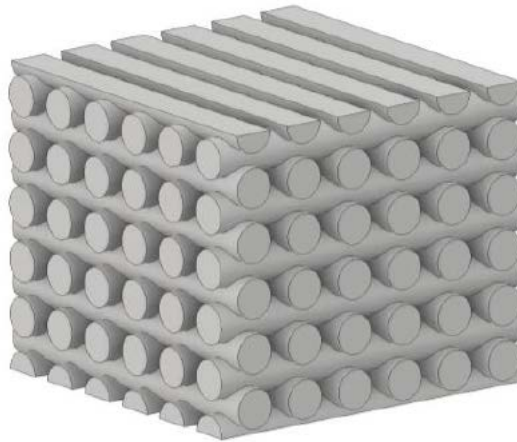


Fig. 1. Layer-by-layer deposition scheme

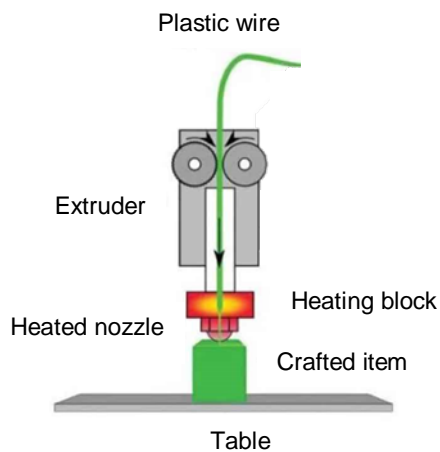


Fig. 2. FDM printing scheme

The most commonly used FDM materials are PLA (polylactide), ABS (acrylonitrile-butadiene-styrene), and PET-G (glycol-doped polyethylene terephthalate) [Kechagias et al. 2023]. PET-G features good elasticity and mechanical strength, by which parts made from this material are less prone to fracture. 3D printing from PET-G is relatively easy. It is a modified version of standard PET (polyethylene terephthalate) [Sathish Kumar et al. 2021]. PET-G sees applications in many areas:

- prototyping;
- fabrication of mechanical parts;
- external features (due to resistance to moisture and UV radiation).

Despite the increasing popularity of PET-G use in FDM, its strength properties vary with the printing process parameters. The nozzle temperature and printing angle significantly affect the mechanical strength and durability of printed parts. A key problem is understanding how these variables affect the quality and mechanical properties of PET-G prints in order to optimise the parts and endow them with better strength. The results of this work can be of particular relevance for engineering and industrial applications.

2. RESEARCH METHODOLOGY

A 1.75mm PET-G filament, purchased from Fiberlogy, was used to fabricate the specimens. The specimens (Fig. 3) were fabricated with preset parameters (Tab. 1) and based on the change in printing angle (Fig. 4) and printing temperature [Alarifi 2023]. The Original Prusa iMK3S+ 3D printer was used to fabricate the specimens (Fig. 5). Static tensile test specimens were fabricated in conformity with PN-ISO 5893:2015-12 [Kończewicz et al. 2022; Krawulski and Dyl 2023] (Fig. 6) in five copies of each printing angle used (0° , 15° , 30° , 45° , 60° , 75° , 90°) per each test temperature (230°C and 250°C). The laboratory static tensile tests were performed on a Zwick & Roell 100 kN testing machine. The results are read in arithmetic mean values.

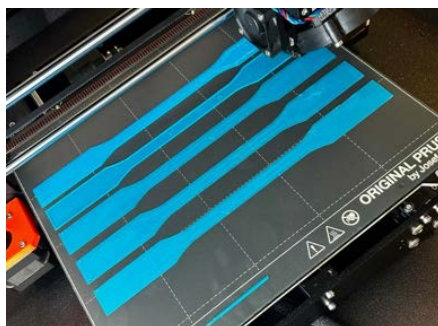


Fig. 3. Samples shown during printing

Table 1. Applied printing parameters

Layer height [mm]	0.2	
No. of outlines	3	
Bottom layer number	3	
Top layer number	3	
Fill ratio [%]	20	
Fill type	Parallel line	
Build platform temperature [°C]	80	
Nozzle temperature [°C]	230	250
Top coat pattern	Mono	

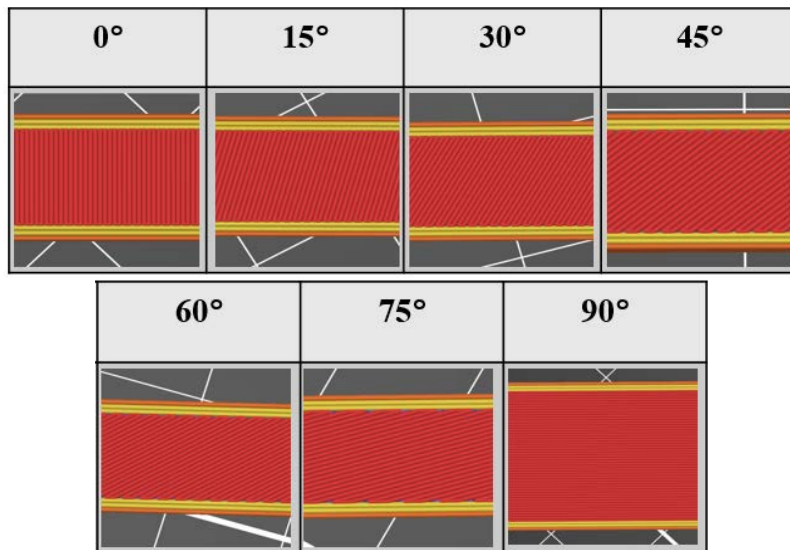


Fig. 4. Method of specimen printing layer angle change



Fig. 5. Original Prusa i3 MK3S+ 3D printer

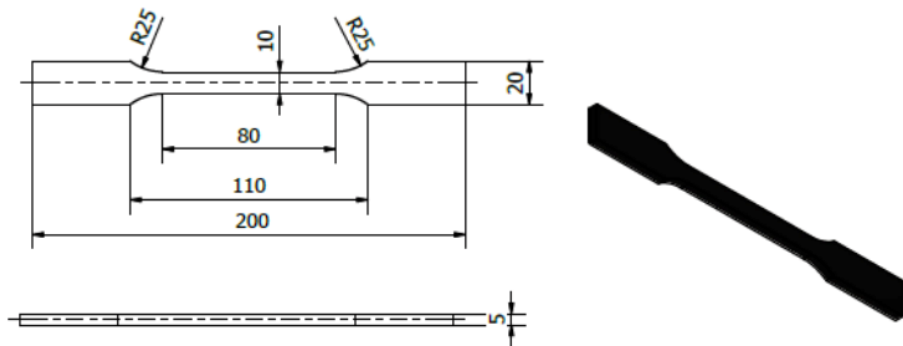


Fig. 6. Dimensions of strength test specimens

3. TEST RESULTS

The graph (Fig. 7) shows the measured results of Young's modulus versus printing angle of the samples at 230°C.

Table 2 lists the Young's modulus values and printing time per one specimen.

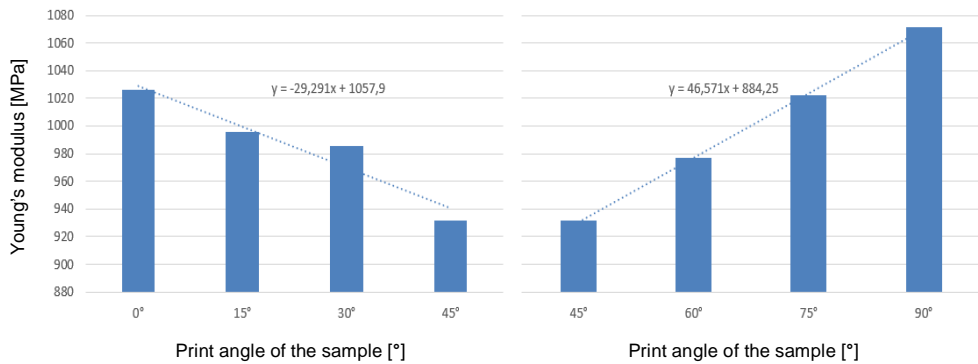


Fig. 7. Young's modulus vs. printing angle change graph

Table 2. Summary of test results for the Young's modulus and printing time per specimen printing angle

Printing angle [°]	0	15	30	45	60	75	90
Young's modulus [MPa]	1026	995	986	932	977	1023	1072
Printing time / 1 pc. [min].	49	50	50	52	50	50	49

The highest Young's modulus value and the shortest printing time were achieved for specimens printed at 90°. The lowest Young's modulus value and the longest printing time were achieved for specimens printed at 45°. It was because that the 45° printed specimens were not aligned with the direction of tension, which directly affected the resulting strength performance. The longer printing time was due to the unfavourable angle as far as the nozzle was concerned, which directly affected the length of time it took to print one specimen.

The graph (Fig. 8) shows the results for the tensile strength Rm [MPa] versus the specimen printing angle.

The tensile strength values are listed in Table 3.

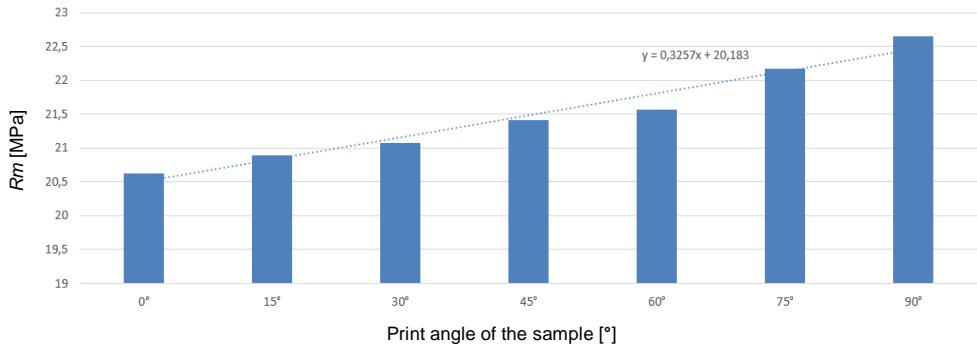


Fig. 8. Tensile strength vs. printing angle change graph

Table 3. Summary of test results for tensile strength Rm [MPa]

Printing angle [°]	0	15	30	45	60	75	90
Tensile strength Rm [MPa]	20.63	20.89	21.07	21.42	21.57	22.17	22.65

An analysis of the test results achieved revealed a noticeable effect of the printing angle on the tensile strength. Although these values range from approximately 21 to 23 MPa, the highest tensile strength values are those of the specimen printed at 90°, while the lowest are those at 0°. This is directly related to the direction of tension of the specimens, so it is important to verify the use of structural components along with the direction of loading when printing specimens.

The graph (Fig. 9) shows the results for the strain [%] versus the specimen printing angle.

The strain values are listed in Table 4.

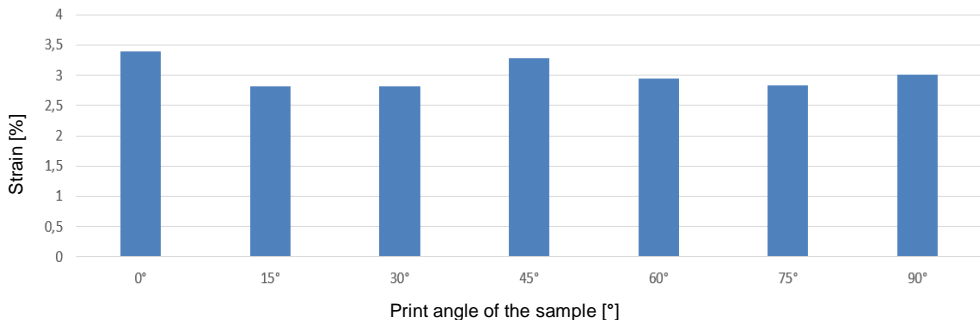


Fig. 9. Strain vs. printing angle change graph

Table 4. Summary of test results for strain

Printing angle [°]	0	15	30	45	60	75	90
Strain [%]	3.39	2.82	2.82	3.29	2.95	2.83	3.01

A relationship was found for strain by which similar and comparable results were produced at printing angles of 0°, 45° and 90°. The least favourable strain results were achieved for printing angles of 15°, 30°, 60° and 75°.

The graph (Fig. 10) shows the measured results of Young’s modulus versus printing angle of the samples at 250°C.

Table 2 lists the Young’s modulus values and printing time per one specimen. Table 5 lists the Young’s modulus values and printing time per one specimen.

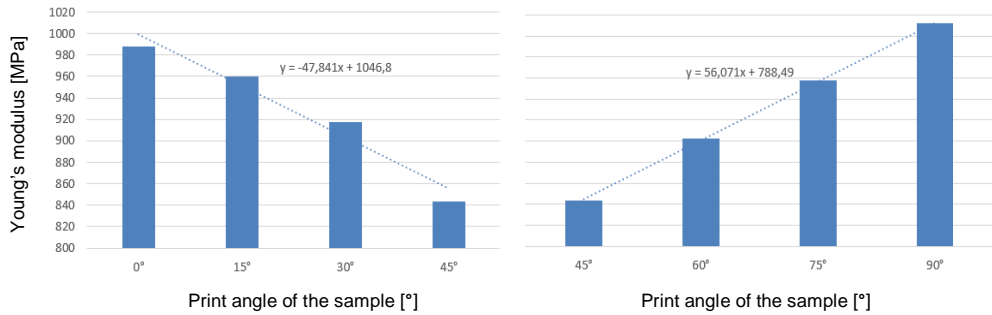


Fig. 10. Young’s modulus vs. printing angle change graph

Table 5. Summary of test results for the Young’s modulus and printing time per specimen printing angle

Printing angle [°]	0	15	30	45	60	75	90
Young’s modulus [MPa]	988	960	917	843	902	957	1012
Printing time / 1 pc. [min].	49	50	50	52	50	50	49

The highest Young’s modulus value and the shortest printing time were achieved for specimens printed at 90°. The lowest Young’s modulus value and the longest printing time were achieved for specimens printed at 45°.

The graph (Fig. 11) shows the results for the tensile strength R_m [MPa] versus the specimen printing angle.

The tensile strength values are listed in Table 6.

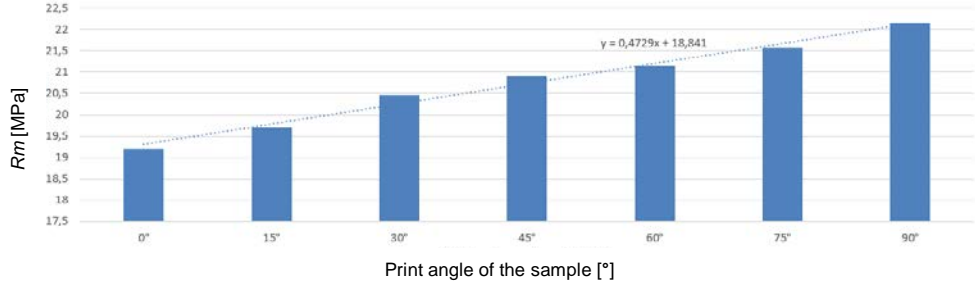


Fig. 11. Tensile strength vs. printing angle change graph

Table 6. Summary of test results for tensile strength R_m [MPa]

Printing angle [°]	0	15	30	45	60	75	90
Tensile strength R_m [MPa]	19.21	19.71	20.46	20.89	21.13	21.57	22.16

The highest tensile strength, R_m was achieved by the specimens printed at 90°. The lowest tensile strength, R_m was achieved by the specimens printed at 0°.

The graph (Fig. 12) shows the results for the strain [%] versus the specimen printing angle.

The strain values are listed in Table 7.

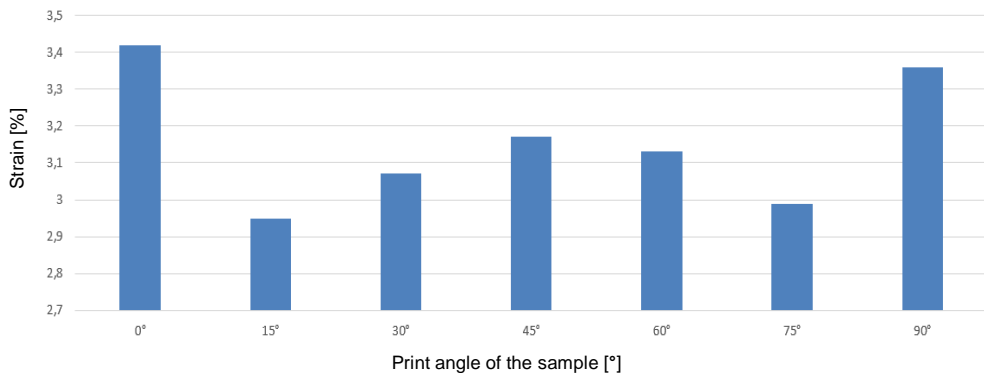


Fig. 12. Strain vs. printing angle change graph

Table 7. Summary of test results for strain

Printing angle [°]	0	15	30	45	60	75	90
Strain [%]	3.42	2.95	3.07	3.17	3.13	2.99	3.36

Table 8 lists the test results obtained for the specimens as a function of changes in the printing angle and temperature.

Table 8. Specimen test results vs. changes in printing angle and temperature

Printing angle	Young's modulus [MPa]		Rm [MPa]		Strain [%]	
	Nozzle temperature		Nozzle temperature		Nozzle temperature	
	230°C	250°C	230°C	250°C	230°C	250°C
0°	1026	988	20.63	19.21	3.39	3.42
15°	995	960	20.89	19.71	2.82	2.95
30°	986	917	21.07	20.46	2.82	3.07
45°	932	843	21.42	20.89	3.29	3.17
60°	977	902	21.57	21.13	2.95	3.13
75°	1023	957	22.17	21.57	2.83	2.99
90°	1072	1012	22.65	22.16	3.01	3.36

The graph (Fig. 13) is a comparison of the test results for Young's modulus.

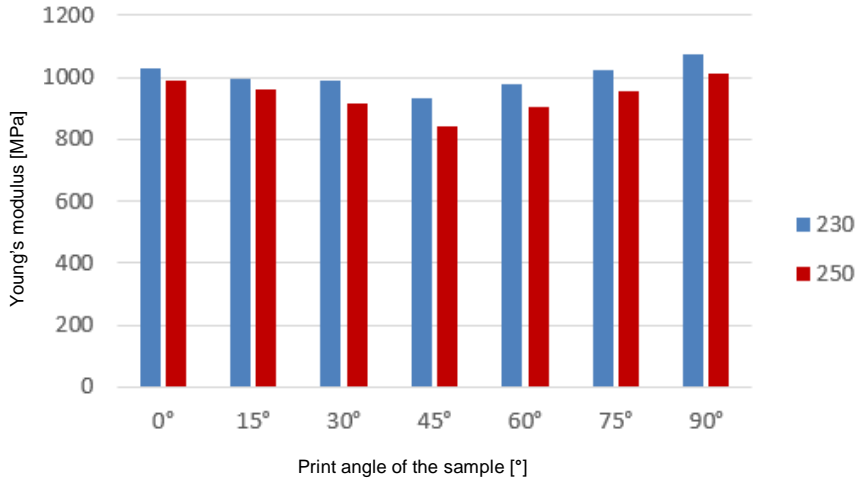


Fig. 13. Young's modulus comparison graph

The graph (Fig. 14) is a comparison of the test results for tensile strength.

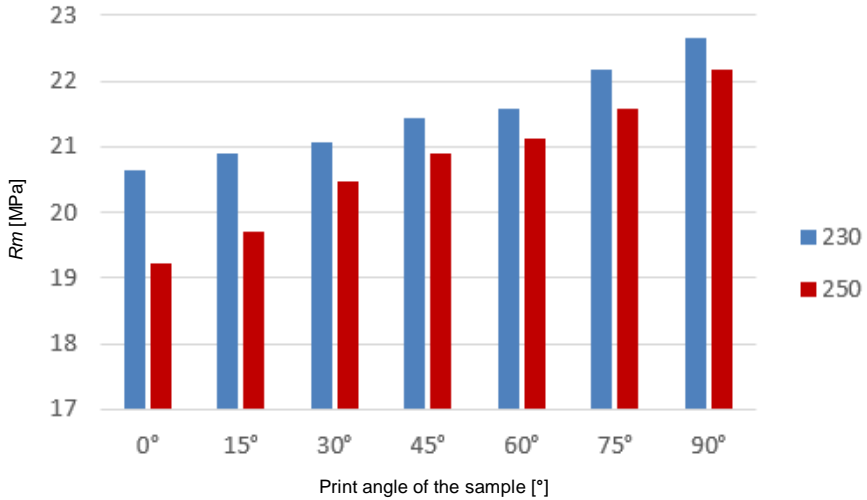


Fig. 14. Tensile strength comparison graph

4. CONCLUSIONS

The specimens tensile-tested in the direction along the fibres (90°) achieved the highest value of Young's modulus. The highest tensile strength value, R_m , was achieved by the specimens printed at an angle of 90° and 230°C.

The temperature and printing angle had a negligible effect on the strain, as the strain test results ranged from 2.82% to 3.42%. The analysis of the test results revealed that the highest strain was in the specimens printed at 0°, 45° and 90° at the tested printing temperatures.

The shortest printing time and also the best strength properties of PET-G were achieved in the specimens printed at 90° and 230°C.

The tests showed that the orientation angle of fibres (rasters) and the printing temperature affected the strength properties.

The analysis of the test results allowed to determine the optimum selection of 3D printing parameters which could contribute to further investigations into the optimisation of FDM fabrication from PET-G.

REFERENCES

- Alarifi, I.M., 2023, *Mechanical Properties and Numerical Simulation of FDM 3D Printed PETG/Carbon Composite Unit Structures*, Journal of Materials Research and Technology, vol. 23, pp. 656–669.
- Fountas, N.A., Papantoniou, I., Kechagias, J.D., Manolagos, D.E., Vaxevanidis, N.M., 2022, *Modeling and Optimization of Flexural Properties of FDM-Processed PET-G Specimens Using RSM and GWO Algorithm*, Engineering Failure Analysis, vol. 138.
- Kechagias, J.D., Fountas, N.A., Ninikas, K., Petousis, M., Vidakis, N., Naxevanidis, N., 2023, *Surface Characteristics Investigation of 3D-Printed PET-G Plates During CO₂ Laser Cutting*, Additive Manufacturing and 3D Printing, vol. 37, pp 1347–1357.
- Kończewicz, W., Krawulski, P., Bieszk, A., Darznik, D., 2022, *The Analysis of Properties Selected Filaments for Making Components and Parts of Marine Equipment by Fused Deposition Modelling on Example of Flexible Clutch Coupling and Oil Centrifuge Scroll*, Journal of Konbin, vol. 52(3), pp. 211–221.
- Krawulski, P., Dyl, T., 2023, *The Impact of 3D Printing Assumptions and CNC Machining Conditions on the Mechanical Parameters of the Selected PET Material*, Archives of Materials Science and Engineering, vol. 120, pp. 36–41.
- Kumaresan, R., Samykano, M., Kadirgama, K., Pandey, A.K., Rahman, Md. M., 2023, *Effects of Printing Parameters on the Mechanical Characteristics and Mathematical Modelling of FDM-Printed PETG*, The International Journal of Advanced Manufacturing Technology, vol. 128, pp. 3471–3489.
- Popescu, D., Zapciu, A., Amza, C., Baci, F., Marinescu, R., 2018, *FDM Process Parameters Influence Over the Mechanical Properties of Polymer Specimens*, Polymer Testing, vol. 69, pp. 157–166.
- Sathish Kumar, K., Soundararajan, R., Shanthosh, G., Saravanakumar, P., Ratteesh, M., 2021, *Augmenting Effect of Infill Density and Annealing on Mechanical Properties of PETG and CFPETG Composites Fabricated by FDM*, Materials Today, vol. 45, pp. 2186–2191.

- Soleyman, E., Aberoumand, M., Soltanmohammadi, K., Rahmatabadi, D., Ghasemi, I., Baniassadi, M., Abrinia, K., Baghani, M., 2022, *4D Printing of PET-G Via FDM Including Tailormade Excess Third Shape*, Manufacturing Letters, vol. 33, pp. 1–4.
- Szykiedans, K., Credo, W., Osiński, D., 2017, *Selected Mechanical Properties of PETG 3-D Prints*, Procedia Engineering, vol. 177, pp. 455–461.
- Zisopol, D.G., Minescu, M., Iacob, D.V., 2023, *A Study on the Evaluation of the Compression Behavior of PLA Lattice Structures Manufactured by FDM*, Engineering, Technology & Applied Science Research, vol. 13, pp. 11 801–11 806.

The article is available in open access and licensed under a Creative Commons Attribution 4.0 International (CC BY 4.0).